ResearchGate

See discussions, stats, and author profiles for this publication at: https://www.researchgate.net/publication/231455375

# Detailed studies of propagating fronts in the iodate oxidation of arsenous acid

**ARTICLE** *in* JOURNAL OF THE AMERICAN CHEMICAL SOCIETY · JULY 1982

Impact Factor: 12.11 · DOI: 10.1021/ja00378a011

CITATIONS
120

READS
32

**3 AUTHORS**, INCLUDING:

Alan Saul
Georgia Regents University
**30** PUBLICATIONS **950** CITATIONS
SEE PROFILE

Kenneth Showalter
West Virginia University
**124** PUBLICATIONS **5,630** CITATIONS
SEE PROFILE

Available from: Alan Saul
Retrieved on: 25 January 2016

# Detailed Studies of Propagating Fronts in the Iodate Oxidation of Arsenous Acid

**Adel Hanna, Alan Saul, and Kenneth Showalter***

*Contribution from the Department of Chemistry, West Virginia University, Morgantown, West Virginia 26506.* *Received November 23, 1981*

**Abstract:** In an unstirred thin film of solution containing iodate and arsenous acid, a single propagating wave of chemical reactivity may be exhibited. The wave converts the solution from colorless to blue in reaction mixtures containing iodate in stoichiometric excess and starch indicator. The wave appears as a narrow blue band propagating through a colorless solution in reaction mixtures containing arsenous acid in stoichiometric excess. Waves were electrochemically initiated and propagation velocity was measured as a function of reactant concentrations. Iodide concentration was measured with an iodide selective microelectrode as a wave passed through the electrode position. The reaction-diffusion behavior is explained with a simple reaction mechanism autocatalytic in iodide.

The coupling of chemical reaction with diffusion may give rise to propagating chemical waves, provided the reaction contains some appropriate form of kinetic feedback such as autocatalysis. Two fundamentally different types of reaction-diffusion waves have been observed in isothermal chemical systems: propagating *pulses* and propagating *fronts*.[1]

The chemical waves in the excitable Belousov-Zhabotinsky[2] (BZ) reaction are propagating pulses of reactivity. As a pulse passes through a point, the reaction intermediates undergo a concentration excursion which returns to its original state. In the BZ reaction, reactants are little depleted in an excursion and the pulse therefore effectively regenerates the kinetic state of the solution it passes through.[3] Propagating pulses have also been observed in the recently discovered oscillating iodate-chlorite-malonic acid reaction.[4]

Propagating fronts of chemical reactivity were observed in the iodate oxidation of arsenous acid over 25 years ago by Epik and Shub.[5] In a recent study of this system,[6] the wave behavior was confirmed and a qualitative explanation was proposed. In addition, an electrochemical method for initiating the waves in a thin film of solution was developed. As a front passes through a point the chemical species undergo a concentration excursion; however, instead of returning to their original concentrations, a new kinetic state is generated. A propagating front therefore converts a reaction mixture from one kinetic state to another. In the iodate-arsenous acid reaction, the front converts the reaction mixture from an initial state where very little reaction has occurred to the state of thermodynamic equilibrium. Propagating fronts have also been studied in the bromate oxidation of ferroin.[7]

Net reaction I describes the iodate-arsenous acid reaction when arsenous acid is in stoichiometric excess to iodate ($[As(III)]_0 > 3[IO_3^-]_0$). When iodate is in stoichiometric excess to arsenous acid ($[As(III)]_0 < {}^5/_2[IO_3^-]_0$), the system is described by net reaction II. An appropriate linear combination of (I) and (II)

$$IO_3^- + 3H_3AsO_3 = I^- + 3H_3AsO_4 \quad (I)$$

$$2IO_3^- + 5H_3AsO_3 + 2H^+ = I_2 + 5H_3AsO_4 + H_2O \quad (II)$$

describes the system when the initial reaction mixture contains ${}^5/_2[IO_3^-]_0 < [As(III)]_0 < 3[IO_3^-]_0$.

Table I. Composition of Reaction Mixtures

| reactant (X) | $[X]_0$/M | $[X]_0$/M range for $R \geq 3$ | $[X]_0$/M range for $R < 3$ |
|---|---|---|---|
| $NaIO_3$ | $5.00 \times 10^{-3}$ | $(4.20\text{-}5.00) \times 10^{-3}$ | $(0.60\text{-}1.50) \times 10^{-2}$ |
| $H_3AsO_3$ | $1.55 \times 10^{-2}$ | $(1.55\text{-}5.43) \times 10^{-2}$ | $(0.16\text{-}1.09) \times 10^{-2}$ |
| $H^+$ | $7.1 \times 10^{-3}$ | $(0.8\text{-}12.6) \times 10^{-3}$ | $(0.8\text{-}12.6) \times 10^{-3}$ |

It is instructive to consider the reaction in terms of two component processes: the Dushman reaction[8] (process A) and the Roebuck reaction[9] (process B). In solutions containing excess arsenous acid, the overall reaction is autocatalytic in iodide according to (A) + 3(B) or (I). The rate of process A is dependent on iodide concentration and the iodine product is reduced by the more rapid process B to regenerate iodide; therefore, iodide concentration increases autocatalytically until iodate is completely consumed. Chemical waves in these reaction mixtures (containing starch indicator) appear as thin blue bands. Figure 1 shows a typical wave at 17.6 min that was initiated at ca. 3.7 min after mixing reactants. In solutions containing excess iodate, the reaction proceeds with autocatalytic generation of iodide according to (A) + 3(B) until arsenous acid is nearly consumed. The accumulated iodide is then oxidized to iodine in process A and 2(A) + 5(B) or (II) describes the overall reaction. Chemical waves in these reaction mixtures (containing starch indicator) appear as blue regions consuming the surrounding colorless solution. Figure 2 shows a typical wave at 23.0 min that was initiated at ca. 7.3 min after mixing reactants.

$$IO_3^- + 5I^- + 6H^+ = 3I_2 + 3H_2O \quad (A)$$

$$H_3AsO_3 + I_2 + H_2O = 2I^- + H_3AsO_4 + 2H^+ \quad (B)$$

In this paper, we report on a detailed study of the chemical waves in the iodate-arsenous acid reaction. Front propagation velocities have been measured as a function of reactant concentrations for solutions containing arsenous acid and for solutions containing iodate in stoichiometric excess. Measurements of iodide concentration as a wave passes through a fixed point have been carrried out by using an iodide selective microelectrode. In ad-

(1) Waves may also be categorized by the extent that reaction and diffusion couple (see: Reusser, E. J.; Field, R. J. *J. Am. Chem. Soc.* **1979**, *101*, 1063-1071). Other classifications distinguish between systems containing temperature or concentration gradients. For a complete categorization of the various possible types of chemical waves see: Ortoleva, P.; Ross, J. *J. Chem. Phys.* **1974**, *60*, 5090-5107.

(2) (a) Belousov, B. P. *Sb. Ref. Radiat. Med.* **1959**, *1958*, 145-147. (b) Zhabotinsky, A. M. *Dokl. Akad. Nauk SSSR* **1964**, *157*, 392-395.

(3) Field, R. J.; Noyes, R. M. *J. Am. Chem. Soc.* **1974**, *96*, 2001-2006.

(4) De Kepper, P.; Epstein, I. R.; Kustin, K.; Orbán, M. *J. Phys. Chem.* **1982**, *86*, 170-171.

(5) Epik, P. A.; Shub, N. S. *Dokl. Akad. Nauk SSSR* **1955**, *100*, 503-506.

(6) Gribschaw, T. A.; Showalter, K.; Banville, D. L.; Epstein, I. R. *J. Phys. Chem.* **1981**, *85*, 2152-2155.

(7) Chemical waves in the ferroin-bromate system (Showalter, K. *J. Phys. Chem.* **1981**, *85*, 440-447) are not true fronts because the solution composition ahead of the wave slowly changes as bromide is consumed. Chemical waves in the iodate-arsenous acid system are true fronts in the limit of $[I^-]_0 = 0$ in the initial reaction mixture.

(8) Dushman, S. *J. Phys. Chem.* **1904**, *8*, 453-482.

(9) Roebuck, J. R. *J. Phys. Chem.* **1902**, *6*, 365-398.

0002-7863/82/1504-3838$01.25/0 © 1982 American Chemical Society

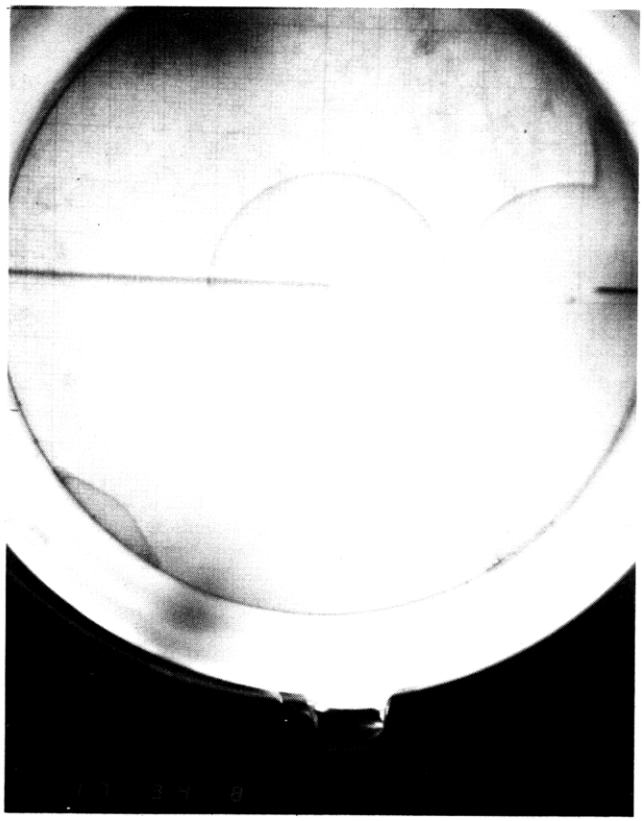

**Figure 1.** Chemical wave in a reaction mixture containing excess arsenous acid. Central wave initiated at negatively biased Pt electrode at ca. 3.7 min and photograph taken at 17.6 min after mixing reactants. Solution composition $[X]_0$ in Table I. Petri dish diameter: 12.5 cm.

dition, we propose a simple model to account for our experimental observations.

## Experimental Section

**Materials and Equipment.** Solutions were prepared with reagent grade chemicals and doubly distilled water. Arsenous acid solution was prepared with $NaAsO_2$ and $H_2SO_4$ in a 1:1 mole ratio. The As(III) concentration was determined by titration with iodine solution according to a standard procedure.[10] Iodate concentration was determined by weight of dissolved chemical.

Chemical wave studies were carried out in a petri dish with a plate glass bottom, thermostated at 25.0 ± 0.2 °C by a water jacket. A Plexiglas cover for the petri dish prevented disturbance of the reaction mixture by air currents. The cover also served as a holder for the wave initiation electrodes (Pt wire, B&S Gauge No. 26), an iodide selective microelectrode (Lazar Research Lab Inc.), and a double junction reference electrode (Orion).

**Procedure.** Reaction mixtures were prepared by pipetting appropriate volumes of stock solutions. The $NaIO_3$ reagent was added last by rapid delivery pipet and complete delivery was defined as time zero. The reaction mixture was thoroughly mixed and spread over the bottom of the petri dish, and the electrodes were positioned.

For investigation of wave velocity dependence on reactant concentrations, one reactant concentration was varied while the other reactant concentrations were held constant. Reactant concentrations and concentration ranges are given in Table I. In all experiments, the reaction mixtures contained 0.04% starch indicator and $8 \times 10^{-4}$ M sodium lauryl sulfate, which facilitated spreading of the solution in the petri dish. Solution acidity was maintained constant by adding a buffer solution prepared by mixing appropriate mole ratios of $NaHSO_4$ and $Na_2SO_4$. Hydrogen ion concentrations were determined by pH measurements. The 10.0-mL reaction mixture generated a solution depth of 0.8 mm in the petri dish.

Waves were initiated at a Pt electrode in the center of the dish negatively biased at −1.0 V with respect to a Pt electrode near the edge of the dish. The electrodes were positioned and the power supply was turned on 1.5 min after time zero. The power supply was turned off at the first appearance of a dark film of solution surrounding the Pt electrode, signaling the initiation of a wave. Wave front position as a function of time was recorded by taking photographs at timed intervals.

Measurements of iodide concentration were made with an iodide selective microelectrode positioned 19 mm from the Pt initiation electrode. Iodide concentration was measured as a function of time as a wave passed through the electrode position. Other measurements of iodide concentration in stirred reaction mixtures were made with the same electrode.

(10) Skoog, D. A.; West, D. M. "Analytical Chemistry", 3rd ed.; Holt, Rinehart and Winston: New York, 1979.

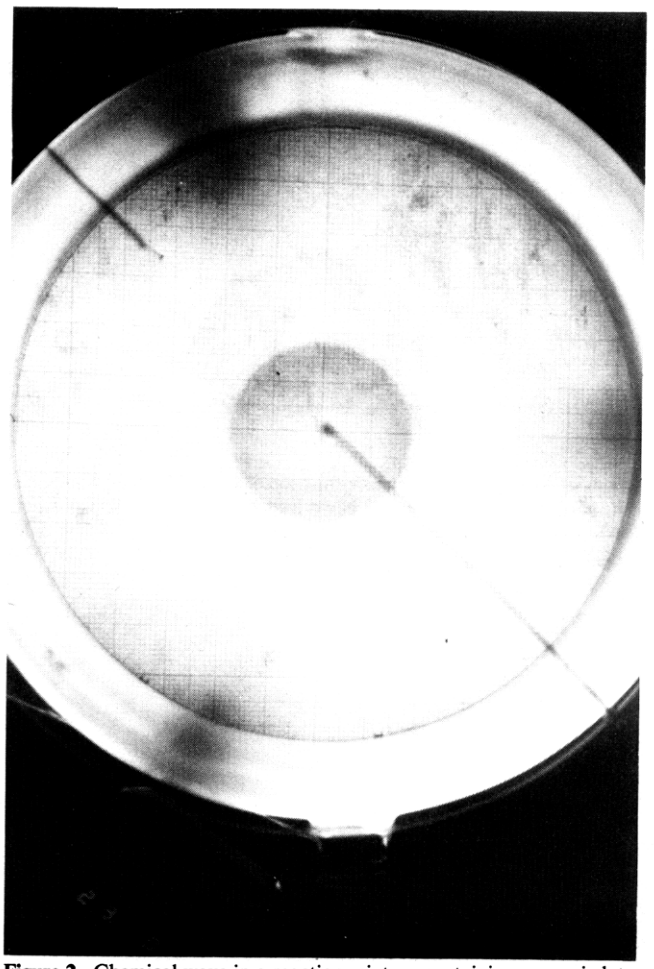

**Figure 2.** Chemical wave in a reaction mixture containing excess iodate. Wave initiated at negatively biased Pt electrode at ca. 7.3 min and photograph taken at 23.0 min after mixing reactants. Solution composition: $[NaIO_3]_0 = 5.00 \times 10^{-3}$ M, $[H_3AsO_3]_0 = 3.16 \times 10^{-3}$ M, $[H^+]_0 = 3.76 \times 10^{-3}$ M.

## Results

The ratio of the initial arsenous acid concentration to the initial iodate concentration, $R = [H_3AsO_3]_0/[IO_3^-]_0$, determines which type of chemical wave is exhibited in the iodate–arsenous acid system. Plots of wave front position as a function of time were linear for reaction mixtures with $R \geq 3$. The circles in Figure 3 show distance vs. time data for two reaction mixtures differing only in $[H_3AsO_3]_0$. The solid lines show linear least-squares fits of the data. Therefore, waves propagate with constant velocity in these reaction mixtures. Plots of wave position as a function of time were approximately exponential for reaction mixtures with $R < 3$. The triangles in Figure 3 show distance vs. time data for two reaction mixtures differing only in $[H_3AsO_3]_0$. The dashed lines show exponential least-squares fits of the data. Therefore, wave velocity increases exponentially in time for these reaction mixtures.

**Effect of Reactant Concentrations on Wave Propagation for $R \geq 3$.** Three series of experiments were carried out to determine the effect of initial reactant concentrations on wave velocity for reaction mixtures containing excess $H_3AsO_3$. A linear dependence of wave velocity on iodate concentration is shown in Figure 4. Only a narrow range of iodate concentrations could be studied in this series of experiments because at concentrations lower than

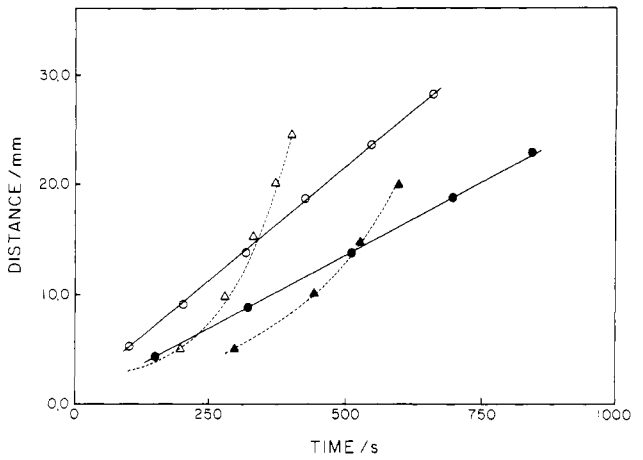


**Figure 3.** Wave front position as a function of time for reaction mixtures containing excess arsenous acid (solid lines) and excess iodate (dashed lines). Solution composition $[X]_0$ in Table I except $[H_3AsO_3]_0 = 5.43 \times 10^{-2}$ M (○), $3.10 \times 10^{-2}$ M (●), $1.09 \times 10^{-2}$ M (△), $4.65 \times 10^{-3}$ M (▲).

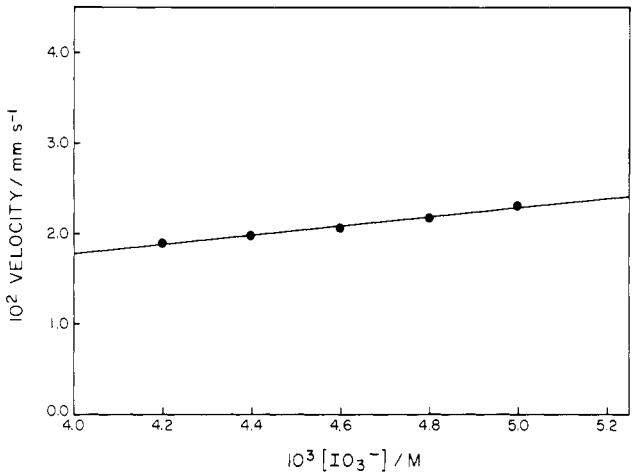


**Figure 4.** Wave velocity as a function of $[IO_3^-]_0$ in solutions containing excess arsenous acid. Solution compositions in Table I.

**Table II.** Effect of Solution Composition on Wave Velocity for $R \geq 3$

| reactant (X) varied | $(dv/d[X]_0)$/ mm $s^{-1}$ $M^{-1}$ | $10^2[X]_0(dv/d[X]_0)$/mm $s^{-1}$ |
|---|---|---|
| $NaIO_3$ | 5.049 | 2.525 |
| $H_3AsO_3$ | 0.479 | 0.742 |
| $H^+$ | 1.93 | 1.36 |

those in Table I, waves were not initiated at the Pt electrode. A linear velocity dependence on arsenous acid concentration is shown in Figure 5. In Figure 6, a linear velocity dependence on hydrogen ion concentration is shown. In this series of experiments, different solution acidities were obtained by varying the $NaHSO_4/Na_2SO_4$ ratio in the buffer solution.

The solid lines in Figures 4–6 show linear least-squares fits of the data. The slopes are given in Table II. Also given in Table II are the relative slopes, obtained by multiplying the slope in each case by the concentration at which the reactant was held constant in the other experiments. The relative slopes indicate that wave velocity depends primarily on $[H^+]_0$ and $[IO_3^-]_0$.

**Effect of Reactant Concentrations on Wave Propagation for $R < 3$.** Three series of experiments were carried out to determine wave velocity dependence on initial reactant concentrations for reaction mixtures containing excess $IO_3^-$. Least-squares fits of the approximately exponential plots of distance vs. time generated the regression constants $a$ and $b$ in eq 1 for each experiment. The

$$x = ae^{bt} \tag{1}$$

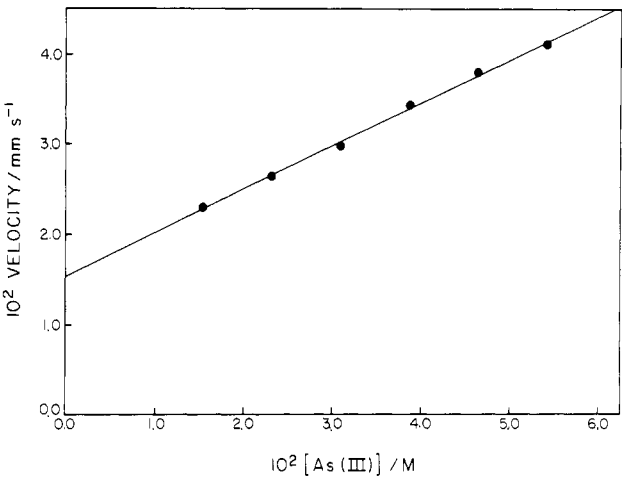


**Figure 5.** Wave velocity as a function of $[H_3AsO_3]_0$ in solutions containing excess arsenous acid. Solution compositions in Table I.

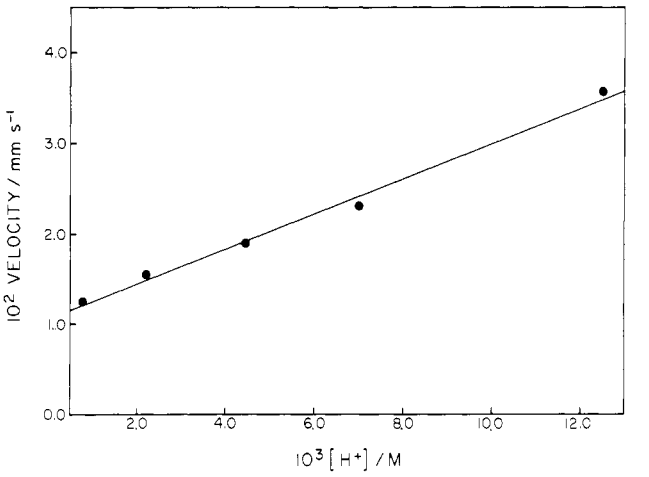


**Figure 6.** Wave velocity as a function of $[H^+]_0$ in solutions containing excess arsenous acid. Solution compositions in Table I.

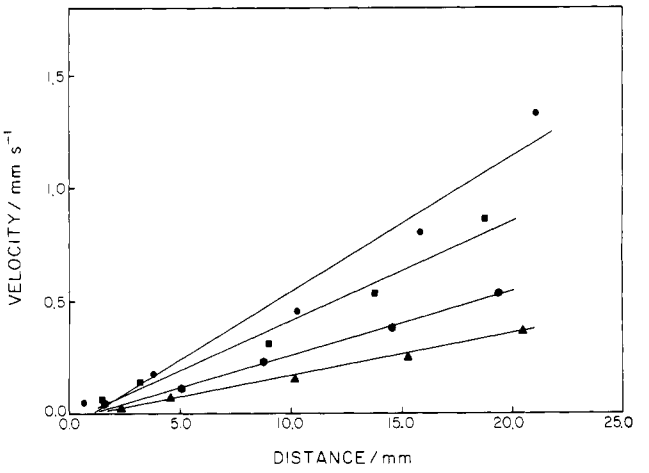


**Figure 7.** Wave velocity as a function of distance for different $[IO_3^-]_0$ in solutions containing excess iodate. Solution composition $[X]_0$ in Table I except $[IO_3^-]_0 = 6.00 \times 10^{-3}$ M (▲), $7.00 \times 10^{-3}$ M (●), $1.00 \times 10^{-2}$ M (■), $1.50 \times 10^{-2}$ M (●).

time derivative of (1) allows the instantaneous velocity at any time to be determined.

$$v = dx/dt = abe^{bt} = bx \tag{2}$$

We also see that the velocity is a linear function of distance.

Figures 7–9 show velocity as a function of wave front position for different concentrations of the varied reactant. The velocity,

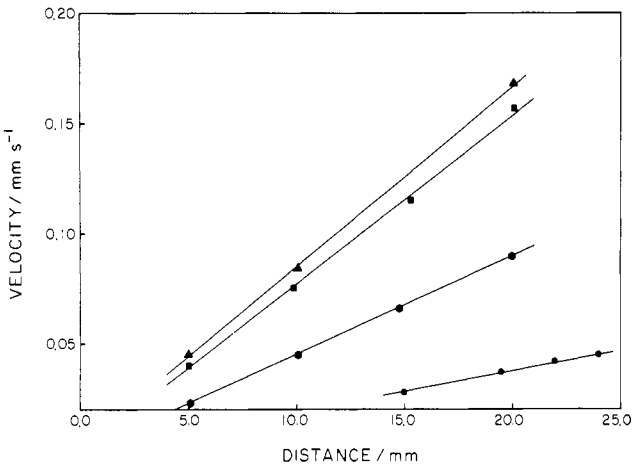


**Figure 8.** Wave velocity as a function of distance for different $[H_3AsO_3]_0$ in solutions containing excess iodate. Solution composition $[X]_0$ in Table I except $[H_3AsO_3]_0 = 1.55 \times 10^{-3}$ M (●), $4.65 \times 10^{-3}$ M (●), $7.75 \times 10^{-3}$ M (■), $1.09 \times 10^{-2}$ M (▲).

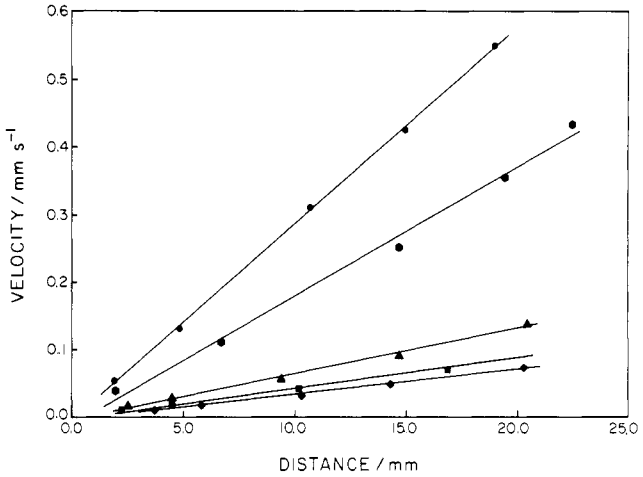


**Figure 9.** Wave velocity as a function of distance for different $[H^+]_0$ in solutions containing excess iodate. Solution composition $[X]_0$ in Table I except $[H^+]_0 = 7.94 \times 10^{-4}$ M (♦), $2.24 \times 10^{-3}$ M (■), $4.47 \times 10^{-3}$ M (▲), $1.26 \times 10^{-2}$ M (●), $2.00 \times 10^{-2}$ M (●).

**Table III.** Effect of Solution Composition on Wave Velocity for $R < 3$

| $10^3[IO_3^-]$/ M | $10^2b$/ $s^{-1}$ | $10^3[H_3AsO_3]$/ M | $10^3b$/ $s^{-1}$ | $10^3[H^+]$/ M | $10^2b$/ $s^{-1}$ |
|---|---|---|---|---|---|
| 6.00 | 1.90 | 1.55 | 1.88 | 0.79 | 0.36 |
| 7.00 | 2.76 | 4.65 | 4.52 | 2.24 | 0.48 |
| 10.00 | 4.39 | 7.75 | 7.67 | 4.47 | 0.69 |
| 15.00 | 6.03 | 10.85 | 9.11 | 12.60 | 1.90 |
| | | | | 20.00 | 2.90 |

calculated at each particular time by using eq 2, is plotted as a function of the corresponding measured distance at that time. Figures 7–9 show that velocity increases at any particular distance with increasing $[IO_3^-]_0$, $[H_3AsO_3]_0$, or $[H^+]_0$. Plots of velocity vs. distance should have zero intercepts according to eq 2. The average intercept (averaged absolute values) in Figures 7–9 is $3.1 \times 10^{-2}$, $1.8 \times 10^{-3}$, and $4.9 \times 10^{-3}$ mm $s^{-1}$, respectively. The least-squares slopes are given in Table III for each concentration of the varied reactant. An approximately linear increase in slope is observed with increasing $[H^+]_0$. At high concentrations of $[IO_3^-]_0$ and $[H_3AsO_3]_0$, the slopes appear to reach a plateau.

**Iodide Concentration Measurements.** Iodide concentration was measured as a function of time as a wave passed through the electrode position. The measurement was made with an iodide selective microelectrode with a sensor tip diameter of about 0.1 mm. The solid curve in Figure 10 shows iodide concentration as

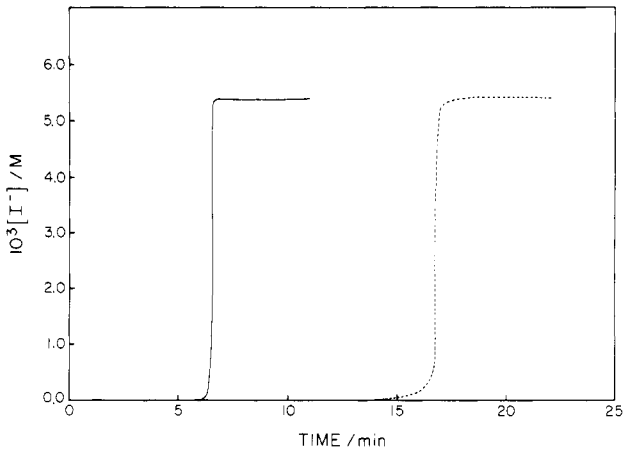


**Figure 10.** Iodide concentration as a function of time in a reaction mixture containing excess arsenous acid. Wave (—) and stirred batch reaction (- - -). Solution composition $[X]_0$ in Table I except $[H_3AsO_3]_0 = 5.43 \times 10^{-2}$ M.

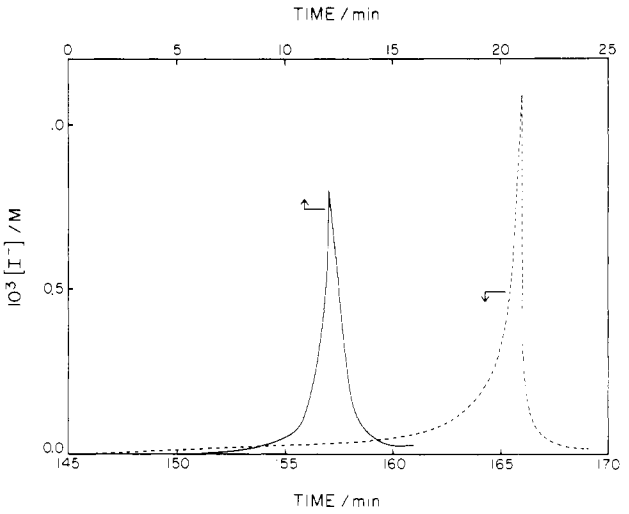


**Figure 11.** Iodide concentration as a function of time in a reaction mixture containing excess iodate. Wave (—) and stirred batch reaction (- - -). Solution composition $[X]_0$ in Table I except $[H_3AsO_3]_0 = 4.65 \times 10^{-3}$ M.

a function of time for a reaction mixture with $R > 3$. Photographic measurements for a reaction mixture of the same composition generated the linear expression for wave front position $x$/mm = $0.9479 + (4.115 \times 10^{-2})$(t/s) with a coefficient of determination $r^2 = 0.999$. Since the increase in iodide concentration in Figure 10 occurs mainly between 6.2 and 6.6 min, the wave front is about 1.0-mm wide. The photographic measurements predict that the iodide increase should occur at 7.3 min for an electrode position of about 19 mm instead of at 6.4 min as shown in Figure 10. The increase in $[I^-]$ coincided with the visually detectable blue band passing through the microelectrode. The photographs showed the width of the visible blue band to be about 0.4 mm.

For reaction mixtures with $R \geq 3$, the iodide concentration should increase to a value given by the stoichiometric relation $[I^-]_{max} = [IO_3^-]_0$, according to net reaction I. The measured $[I^-]_{max}$ in Figure 10 is about 8% higher than the value of $5.0 \times 10^{-3}$ M expected from stoichiometry. The discrepancy is apparently due to experimental error. Also shown in Figure 10 (dashed line) is the iodide concentration as a function of time in a stirred reaction mixture with the same composition. The measured $[I^-]_{max}$ for the stirred reaction mixture is also about 8% above the value expected from stoichiometry.

Iodide concentration was also measured for waves in reaction mixtures with $R < 3$. The solid line in Figure 11 shows the iodide concentration as a function of time as a wave passed through the microelectrode. The iodide concentration reaches a maximum

and then decreases almost to its original value. The maximum $[I^-]$ recorded as the wave passed through the electrode was $8.0 \times 10^{-4}$ M. If the iodide maximum coincided with the complete consumption of $H_3AsO_3$, then the stiochiometric relation $[I^-]_{max} = {}^1/_3[H_3AsO_3]_0$ would follow from reaction I. The $[I^-]_{max}$ in Figure 11 is about 52% of that expected with the assumption of complete consumption of $H_3AsO_3$. Also shown in Figure 11 (dashed line) is the iodide concentration as a function of time in a stirred reaction mixture of the same composition. In this experiment, $[I^-]_{max} = 1.1 \times 10^{-3}$ M, which is about 71% of that expected if $H_3AsO_3$ was completely consumed at the iodide maximum. The maximum iodide concentration for $R < 3$ is always less than ${}^1/_3$ $[H_3AsO_3]_0$, but as $R$ approaches 3, $[I^-]_{max}$ approaches ${}^1/_3[H_3AsO_3]_0$.

For $R \geq 3$, iodide concentration increases to a constant value given by $[I^-]_{max} = [IO_3^-]_0$, according to net reaction I. For $R < {}^5/_2$, iodide increases to a maximum concentration and is then completely consumed in process A. Iodine concentration increases to a constant value given by the stoichiometric relation $[I_2]_{max} = {}^1/_5[H_3AsO_3]_0$, according to net reaction II. For $3 > R > {}^5/_2$, iodide is only partially consumed after reaching a maximum and the net reaction is given by an appropriately weighted sum of reactions I and II. The stoichiometry given by the combination (I) + (II), or $R = {}^8/_3$, should give the maximum $[I_3^-]$ behind the wave front and therefore generate the darkest expanding blue wave in reaction mixtures containing starch indicator.

**Wave Initiation.** Waves were initiated at both positive and negative Pt electrodes. Iodate is apparently reduced to iodide at the negative electrode. Iodide autocatalysis is accelerated in the local region surrounding the electrode. An elevated iodide concentration results and iodide diffuses into surrounding regions. Autocatalysis is promoted in these regions and the result is a propagating chemical wave. Waves at the positive Pt electrode always appeared after waves were initiated at the negative Pt electrode. Arsenous acid is apparently oxidized at the positive electrode and an increased local concentration of $I_2$ results. Waves also appeared at the edges of the dish. Presumably, $I_2$ from a previous experiment was absorbed into the silicone adhesive at the edges of the dish. Waves are immediately initiated upon addition of either $I_2$ or KI solution to the reaction mixture.[5,6] Iodine is rapidly reduced to iodide in process B and iodide autocatalysis is accelerated.

## Discussion

**Reaction Kinetics and Stoichiometry.** The oxidation of arsenous acid by iodate can be expressed as a combination of the Dushman reaction[8] (process A) and the Roebuck reaction[9] (process B). Liebhafsky and Roe[11] have summarized the many studies of the Dushman reaction. They conclude that the kinetics of the reaction are best described by rate law $\alpha$. The reaction is first order in

$$R_\alpha = \frac{-1}{5}\frac{d[I^-]}{dt} = (k_1 + k_2[I^-])[IO_3^-][H^+]^2[I^-] \qquad (\alpha)$$

iodide at $[I^-]$ less than about $10^{-6}$ M and second order in iodide at higher concentrations. In the iodate–arsenous acid reaction, the iodine generated by the Dushman reaction is reduced to iodide in the Roebuck reaction. In his original study, Roebuck[9] showed that the reduction of $I_2$ by As(III) follows rate law $\beta$. A

$$R_\beta = \frac{-d[I_2]}{dt} = \frac{k_3[I_2][H_3AsO_3]}{[I^-][H^+]} \qquad (\beta)$$

three-term rate law that accounts for the various degrees of protonation of As(III) has been proposed by Pendlebury and Smith.[12] Process B is more rapid than process A and therefore the Dushman reaction is rate determining for the overall reaction. The regeneration of iodide by process B gives rise to autocatalysis in iodide at a rate given by $R_\alpha$.

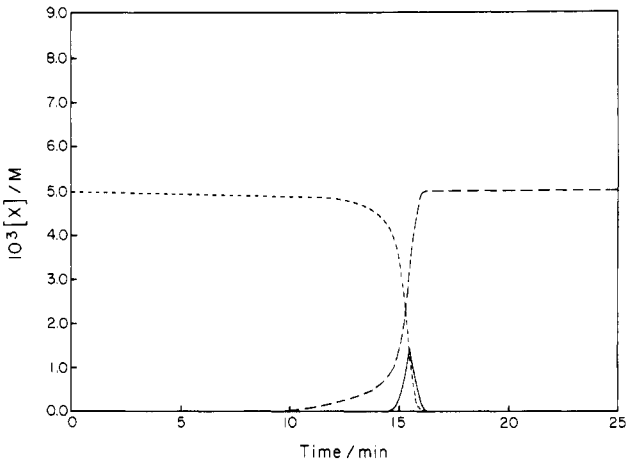


**Figure 12.** Concentrations of $IO_3^-$ (---), $I^-$ (– –), and $I_2$ (—) as a function of time computed from eq R1–4. The concentration of $I_2$ is enlarged by a factor of 350. Initial concentrations: $[IO_3^-]_0 = 5.0 \times 10^{-3}$ M, $[I^-]_0 = 2.5 \times 10^{-5}$ M, $[I_2]_0 = 1.0 \times 10^{-12}$ M. Reactant concentrations held constant: $[H_3AsO_3]_0 = 5.43 \times 10^{-2}$ M, $[H^+]_0 = 7.1 \times 10^{-3}$ M. Rate constants: $k_1 = 4.5 \times 10^3$ $M^{-3}$ $s^{-1}$, $k_2 = 1.0 \times 10^8$ $M^{-4}$ $s^{-1}$, $k_3 = 3.2 \times 10^{-2}$ M $s^{-1}$.

The iodate–arsenous acid reaction has recently been found to exhibit kinetic bistability in a continuous flow stirred tank reactor.[13,14] De Kepper, Epstein, and Kustin[14] successfully modeled the bistability in terms of process A and process B with rate laws $\alpha$ and $\beta$. A detailed mechanism for the reaction consistent with rate laws $\alpha$ and $\beta$ has been proposed[13] which combines the Liebhafsky–Roe[11] mechanism for the Dushman reaction with Roebuck's[9] original mechanism for the reduction of $I_2$ by As(III). Numerical integration of the rate equations generated behavior in good agreement with the experimental behavior.[13]

The kinetic behavior of the homogeneous batch reaction can also be analyzed in terms of process A and process B with rate laws $\alpha$ and $\beta$. Rate equations for each of the species in the rate laws are given by eq R1–4. The concentration of hydrogen ion

$$d[I^-]/dt = -5R_\alpha + 2R_\beta \qquad (R1)$$

$$d[I_2]/dt = 3R_\alpha - R_\beta \qquad (R2)$$

$$d[IO_3^-]/dt = -R_\alpha \qquad (R3)$$

$$d[H_3AsO_3]/dt = -R_\beta \qquad (R4)$$

was maintained constant by buffering the reaction mixtures and therefore it is not included as a variable. In eq R1–4, process A and process B are regarded as irreversible. The reverse reaction in process B may become significant at high As(V) and $I^-$ concentrations; however, this feature was not included in the rate equations in order to minimize the number of variables.

Figure 12 shows the concentrations of $I^-$, $IO_3^-$, and $I_2$ as a function of time computed from eq R1–4.[15] The initial concentrations in the computation correspond to the excess arsenous acid reaction mixture used for Figure 10. Arsenous acid concentration was regarded as constant in the calculation because for this solution composition it is in stoichiometric excess by a factor of 3.6. The rate constants $k_1$ and $k_2$ were taken from Papsin, Hanna, and Showalter.[13] The value used for $k_3$ is near that obtained by Pendlebury and Smith[12] in a study of the Roebuck reaction. The formation constant for $I_3^-$ was absorbed into $k_3$ in order to express rate law $\beta$ in terms of $I_2$. (See figure caption for rate constants.)

In reaction mixtures containing $H_3AsO_3$ in stoichiometric excess, the iodine and oxyiodine intermediates never reach stoi-

(11) Liebhafsky, H. A.; Roe, G. M. *Int. J. Chem. Kinet.* **1979**, *11*, 693–703.
(12) Pendlebury, J. N.; Smith, R. H. *Int. J. Chem. Kinet.* **1974**, *6*, 663–685.
(13) Papsin, G. A.; Hanna, A.; Showalter, K. *J. Phys. Chem.* **1981**, *85*, 2575–2582.
(14) De Kepper, P.; Epstein, I.R.; Kustin, K. *J. Am. Chem. Soc.* **1981**, *103*, 6121–6127.
(15) (a) Hindmarsh, A. C. "Gear: Ordinary Differential Equation Solver", Technical Report No. UCID-30001, Rev. 3; Lawrence Livermore Laboratory: Livermore, CA, 1974. (b) Field, R. J. *J. Chem. Educ.* **1981**, *58*, 408.

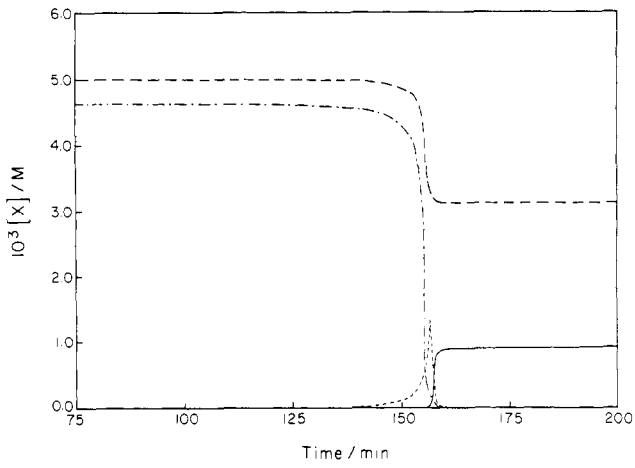


**Figure 13.** Concentrations of $IO_3^-$ (--), $I^-$ (---), $I_2$ (—), and $H_3AsO_3$ (---) as a function of time computed from eq R1–4. Initial concentrations: $[IO_3^-]_0 = 5.0 \times 10^{-3}$ M, $[I^-]_0 = 1.0 \times 10^{-9}$ M, $[I_2]_0 = 1.0 \times 10^{-12}$ M, $[H_3AsO_3]_0 = 4.65 \times 10^{-3}$ M. Reactant concentration held constant: $[H^+] = 7.1 \times 10^{-3}$ M. See Figure 12 for rate constants.

chiometrically significant concentrations. Therefore, the concentrations of iodate and iodide are related by $[IO_3^-]_0 = [IO_3^-] + [I^-]$ according to net reaction I. Even at the $I_2$ maximum in Figure 12, the sum $[IO_3^-] + [I^-]$ is equal to 99.8% of the initial $IO_3^-$ concentration. Spectrophotometric measurements confirmed that $I_2$ never reaches a significant concentration during its transient appearance, although the measured $[I_2]_{max}$ was somewhat higher than the value in Figure 12.[16]

The duration of the induction period was extremely sensitive to the initial concentration of $I^-$. When the calculation in Figure 12 was repeated with the initial $[I^-]$ doubled, the $I_2$ maximum occurred at 9.8 min. Bognár and Sárosi[17] utilized this sensitivity to initial $[I^-]$ to devise an analytical method for determining trace iodide. The initial $[I^-]$ in Figure 12 was arbitrarily adjusted to give an induction period about the same as that in Figure 10.

Figure 13 shows the concentrations of $I^-$, $IO_3^-$, $I_2$, and $H_3AsO_3$ as a function of time computed from eq R1–4. The initial concentrations in this calculation correspond to the excess iodate reaction mixture used for Figure 11. The initial concentration of $I^-$ in the calculation was adjusted so that the induction period was about the same as that in Figure 11. The calculated $[I^-]_{max}$ in Figure 13 ($1.32 \times 10^{-3}$ M) is in good agreement with the measured $[I^-]_{max}$ in Figure 11 ($1.09 \times 10^{-3}$ M). Spectrophotometric measurements confirmed that $[I_2]$ increases as shown in Figure 13 to a value expected from the stoichiometry of net reaction II.[18]

When iodate is in stoichiometric excess, the reaction occurs in two distinct stages. The first stage, from time zero to $[I^-]_{max}$, is similar to the reaction in the presence of excess $H_3AsO_3$. The concentrations of iodide and arsenous acid are related by $[H_3AsO_3]_0 = [H_3AsO_3] + 3[I^-]$ according to net reaction I. In Figure 13, this relation holds to 1% from time zero to 16 s before $[I^-]_{max}$. Even at the $[I^-]$ maximum, $[H_3AsO_3] + 3[I^-]$ is equal to 91.8% of $[H_3AsO_3]_0$. In the second stage of the reaction at times following $[I^-]_{max}$, the accumulated $I^-$ is oxidized to $I_2$ in process A. The concentrations of iodide and iodine are related by $[H_3AsO_3]_0 = 5[I_2] + 3[I^-]$ according to the stoichiometries of process A and net reaction I. This relation holds to 1% for times beyond 5 s after $[I^-]_{max}$. At the $[I^-]$ maximum, $5[I_2] + 3[I^-]$ is equal to 93.3% of $[H_3AsO_3]_0$. Therefore, in solutions containing excess $IO_3^-$, the reaction proceeds with the autocatalytic generation of $I^-$ according to (A) + 3(B) followed by the oxidation of the accumulated $I^-$ according to process A.

**Chemical Waves in Solutions Containing Excess Arsenous Acid.** Waves appear as thin blue bands in reaction mixtures containing $H_3AsO_3$ in stoichiometric excess. The blue band represents the region in the wave front where $I_2$ concentration is sufficient to give the starch indicator color. The $I_2$ reacts rapidly with excess $I^-$ in this region to form $I_3^-$ and the blue starch complex. In the experiments for Figure 5, the bandwidth decreased as the $[H_3AsO_3]_0$ was increased. This effect limited the concentration range in this series of experiments because the wave front became so narrow that it was not visible for $[H_3AsO_3]_0 > 5.43 \times 10^{-2}$ M. Spectrophotometric measurements showed that $[I_2]_{max}$ decreased with increasing $[H_3AsO_3]_0$ in stirred solutions. A decrease in $[I_2]_{max}$ was also observed when the calculation in Figure 12 was repeated with increased $[H_3AsO_3]_0$. The extent that $I_2$ accumulates depends on the relative rates at which it is generated and consumed by process A and process B. The rate of process B is first order in $[H_3AsO_3]$ according to rate law $\beta$ and therefore an increase in $[H_3AsO_3]_0$ tends to diminish the buildup of $I_2$.

Figures 4–6 show that wave velocity is a function of $[IO_3^-]_0$, $[H_3AsO_3]_0$, and $[H^+]_0$. However, the relative slopes of the velocity vs. concentration plots (Table II) indicate that the velocity dependence on $[IO_3^-]_0$ and $[H^+]_0$ is greater than the dependence on $[H_3AsO_3]_0$. Process A is rate determining for iodide autocatalysis and a rate dependence on $[IO_3^-]_0$ and $[H^+]_0$ is expected from rate law $\alpha$. A simple model for the chemical wave may be developed from the rate law for process A when the influence of $[H_3AsO_3]_0$ on the propagation velocity is neglected. The substitution of the stoichiometric relation $[IO_3^-] = [IO_3^-]_0 - [I^-]$ into rate law $\alpha$ allows us to write the reaction–diffusion equation

$$\left(\frac{\partial C}{\partial t}\right)_x = D\left(\frac{\partial^2 C}{\partial x^2}\right)_t + (k_1 + k_2 C)([IO_3^-]_0 - C)[H^+]^2 C \quad (3)$$

where $C = [I^-]$. We now have a single variable model for the system with kinetics which are formally third order. We must assume that $I^-$ and $IO_3^-$ have the same diffusion coefficients in eq 3 for the stoichiometric relation to be valid locally within the wave front.[19] The homogeneous steady states from eq 3 are $-k_1/k_2$, 0, and $[IO_3^-]_0$. Of course the negative root is not physically meaningful. The zero root corresponds to the initial state and the root equal to $[IO_3^-]_0$ corresponds to the concentration of iodide at thermodynamic equilibrium according to net reaction I. A linear stability analysis shows that for the homogeneous system, the negative and positive roots are stable and the zero root is unstable to infinitesimal perturbation. Therefore, the system leaves the unstable initial state upon an infinitesimal increase in $[I^-]$ and proceeds to the stable state of thermodynamic equilibrium.

Figure 3 shows that waves propagate with constant velocity and therefore we may substitute $v = (\partial x/\partial t)_C$ into eq 3 to give the ordinary differential equation

$$D\frac{d^2C}{dx^2} + v\frac{dC}{dx} + (k_1 + k_2 C)([IO_3^-]_0 - C)[H^+]^2 C = 0 \quad (4)$$

A linear stability analysis with respect to $x$ of the first-order system derived from eq 4 shows that the zero root is a stable node and that the positive root is a saddle point. The trajectory connecting these stationary states corresponds to a stable propagating front.[20]

A particular analytical solution of eq 3 or 4 is given by

$$C(x,t) = \frac{[IO_3^-]_0}{1 + Ae^{k(x-vt)}} \quad (5)$$

where

$$k = [IO_3^-]_0[H^+]_0(k_2/2D)^{1/2} \quad (6)$$

$$v = (k_1/k)[IO_3^-]_0[H^+]_0^2 + Dk \quad (7)$$

(16) Measurements at 469 nm gave $[I_2]_{max} = 9.45 \times 10^{-5}$ M with $a = 730$ $M^{-1}$ $cm^{-1}$ (Kern, D. M.; Kim, C. H. *J. Am. Chem. Soc.* **1965**, *87*, 5309–5313) compared to $[I_2]_{max} = 4.15 \times 10^{-6}$ M in Figure 12.

(17) Bognár, J.; Sárosi, S. *Anal. Chim. Acta* **1963**, *29*, 406–414.

(18) Measurements at 469 nm gave $[I_2]_{max} = 1.06 \times 10^{-3}$ M with[16] $a = 730$ $M^{-1}$ $cm^{-1}$ compared to $[I_2]_{max} = 9.30 \times 10^{-4}$ M in Figure 13.

(19) The diffusion coefficients for $I^-$ and $IO_4^-$ are $2.04 \times 10^{-5}$ and $1.42 \times 10^{-5}$ $cm^2$ $s^{-1}$, respectively. The diffusion coefficient for $IO_3^-$ should be about the same as that for $IO_4^-$. The difference in the coefficients for $I^-$ and $IO_3^-$ will result in the increase in $[I^-]$ to be slightly displaced from the decrease in $[IO_3^-]$ within the chemical wave.

(20) Fife, P. C. *Lect. Notes Biomathematics* **1979**, *28*, 84–123.

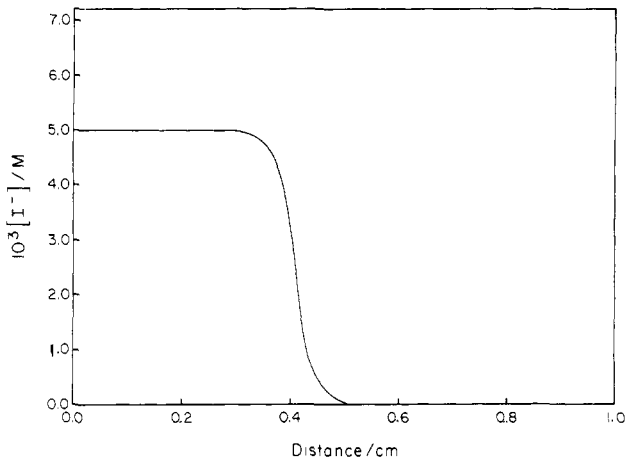


**Figure 14.** Concentration of iodide ($C$) as a function of distance calculated from eq 5 with the arbitrary constant $A = 1.0$, $t = 100$ s, and $D = 2.04 \times 10^{-5}$ cm$^2$ s$^{-1}$. See Figure 10 for initial reactant concentrations and Figure 12 for rate constants.

and $A$ is an arbitrary constant. Figure 14 shows iodide concentration ($C$) as a function of distance calculated from eq 5. The curve represents the change in iodide concentration as the front propagates from left to right in the figure. The concentration change occurs mainly between 3.4 and 4.8 mm, indicating that the front width is about 1.4 mm, in reasonable agreement with the measured width of 1.0 mm in Figure 10. From eq 6 and 7 we calculate $v = 1.15 \times 10^{-2}$ mm s$^{-1}$ for the initial concentrations in Figures 10 and 14. The calculated velocity is low by a factor of 3.6 compared to the experimental velocity ($4.12 \times 10^{-2}$ mm s$^{-1}$). Measured velocities for reaction mixtures containing lower initial $H_3AsO_3$ concentrations are in better agreement with the calculated value. For the reaction mixture composition $[X]_0$ in Table I the experimental velocity ($2.30 \times 10^{-2}$ mm s$^{-1}$) differs from the calculated velocity by a factor of 2.

Combining eq 6 and 7 gives an expression for the wave velocity dependence on initial reactant concentrations.

$$v = m[H^+]_0 + n[H^+]_0[IO_3^-]_0 \quad (8)$$

where $m = k_1(2D/k_2)^{1/2} = 2.87 \times 10^{-2}$ mm s$^{-1}$ M$^{-1}$ and $n = (k_2D/2)^{1/2} = 3.19 \times 10^2$ mm s$^{-1}$ M$^{-2}$. (See Figure 14 for rate constants and diffusion coefficient.) For the solution composition $[X]_0$ in Table I, the first term in eq 8 accounts for less than 2% of the calculated velocity; therefore, the velocity depends primarily on the product $[H^+]_0[IO_3^-]_0$. The plot of $v$ vs. $[IO_3^-]_0$ in Figure 4 gives $m$ and $n$ values of $-3.40 \times 10^{-1}$ mm s$^{-1}$ M$^{-1}$ and $7.11 \times 10^2$ mm s$^{-1}$ M$^{-2}$, respectively. Therefore, the coefficient of the dominant term in eq 8 is low by a factor of 2.2. Disregarding the nonzero intercept of the plot of $v$ vs. $[H^+]_0$ in Figure 5, the slope gives $(m + n[IO_3^-]_0) = 1.93$ mm s$^{-1}$ M$^{-1}$ compared to a value of 1.63 mm s$^{-1}$ M$^{-1}$ from eq 8. The reasonably good agreement with experiment indicates that the essential features of the chemical wave in solutions containing excess $H_3AsO_3$ are accounted for by eq 5.

**Chemical Waves in Solutions Containing Excess Iodate.** Waves appear as expanding regions of blue in reaction mixtures containing iodate in stoichiometric excess. Figure 13 shows that in the homogeneous solution, iodide is autocatalytically generated until $H_3AsO_3$ is almost completely consumed and then the accumulated $I^-$ is oxidized to $I_2$ in process A. The homogeneous system is characterized by two successive stages of reaction. A description of the chemical wave, however, is complicated by the diffusion of $I_2$ ahead in the wave front which results in a secondary coupling of the first and second stages of the reaction.

Figure 3 shows that plots of wave front position vs. time are approximately exponential for reaction mixtures containing excess iodate. Figures 7–9 show that the wave velocity is an approximately linear function of distance and that at any particular distance the velocity increases with an increase in $[IO_3^-]_0$, $[H_3AsO_3]_0$, or $[H^+]_0$. The nonconstant velocity can be rationalized by considering the effects of $I_2$ diffusing ahead in the wave front. Figure 13 shows that $I_2$ is rapidly produced following the maximum in $[I^-]$. According to the stoichiometries of process A and reaction I, the generation of $I_2$ from any particular initial $[I^-]$ proceeds at three times the rate of iodide autocatalysis for the same $[I^-]$, provided that $[IO_3^-]$ is the same in each case. Even when $IO_3^-$ is substantially depleted, as in Figure 13, the increase in $[I^-]$ is followed by a more rapid increase in $[I_2]$. In the chemical wave, the rapid increase in $[I_2]$ gives rise to a steep concentration gradient and $I_2$ diffuses ahead in the wave front. Two $I^-$ are generated from every $I_2$ that diffuses ahead into solution yet containing a significant concentration of $H_3AsO_3$. Iodide autocatalysis is promoted by this additional input of $I^-$ and the consumption of $H_3AsO_3$ is accelerated. The rapid increase in $[I_2]$ therefore occurs earlier, which in turn gives rise to additional diffusion of $I_2$ ahead. This process results in a diffusion-dependent autocatalytic feedback superimposed on the autocatalytic production of $I^-$ by (A) + 3(B). Therefore, the farther the wave propagates, the greater is its propagation velocity.

Process A is rate determining for iodide autocatalysis. Therefore, an increase in velocity at a particular distance with an increase in $[IO_3^-]_0$ or $[H^+]_0$ is expected from rate law $\alpha$. When $H_3AsO_3$ is consumed to a critical concentration, the rates of process A and process B become equal. Iodide autocatalysis is not possible at $H_3AsO_3$ concentrations below the critical concentration and the reaction proceeds with the simple oxidation of accumulated $I^-$. The extent of iodide autocatalysis in the first stage of the reaction depends on the initial $H_3AsO_3$ concentration. The greater the $[H_3AsO_3]_0$, the larger the maximum $[I^-]$ and the subsequent rise in $[I_2]$. Therefore, an increase in $[H_3AsO_3]_0$ results in a greater velocity because the extent of iodide autocatalysis is increased and more $I_2$ is subsequently generated.

## Conclusion

The propagating front in the iodate–arsenous acid system partitions the reaction mixture into two very different kinetic states. The kinetic state of the region ahead of the front resembles the state of the initial reaction mixture. The kinetic state of the region behind the front corresponds to the state of thermodynamic equilibrium. The reaction exhibits similar kinetic states in a continuous flow stirred tank reactor.[13,14] For a range of reactor residence times, the system may exist in one of two possible steady states. One steady state resembles the composition of the initial reaction mixture and the other resembles the composition at thermodynamic equilibrium. Each of the steady states is stable to infinitesimal perturbation and therefore the system exhibits kinetic bistability. In contrast, the unstirred batch system is necessarily monostable with the stable state being thermodynamic equilibrium. However, an initial reaction mixture containing no iodide will remain in that state until iodide is introduced.[21] The dynamic simplicity of the iodate–arsenous acid reaction makes it an attractive system for examining the relationship between kinetic bistability and chemical wave behavior. In a following paper, we will consider the various kinetic behaviors of this reaction and the relations between these behaviors.

**Acknowledgment.** This work was supported by the National Science Foundation (Grant No. ISP-8011453-10) and the donors of the Petroleum Research Fund, administered by the American Chemical Society.

**Registry No.** $H_3AsO_3$, 13464-58-9; $IO_3^-$, 15454-31-6.

(21) Iodate reagent will always contain some iodide; however, in the limit of pure iodate, no reaction is possible. (We assume that no direct reaction between iodate and arsenous acid occurs.)